Bioorganic & Medicinal Chemistry 19 (2011) 5012–5022

Contents lists available at ScienceDirect

Bioorganic & Medicinal Chemistry

journal homepage: www.elsevier.com/locate/bmc

The combination of 4-anilinoquinazoline and cinnamic acid: A novel mode of binding to the epidermal growth factor receptor tyrosine kinase

Dong-Dong Li [a,†], Peng-Cheng Lv [a,†], Hui Zhang [a], Hong-Jia Zhang [a], Ya-Ping Hou [a], Kai Liu [a], Yong-Hao Ye [b,*], Hai-Liang Zhu [a,*]

[a] State Key Laboratory of Pharmaceutical Biotechnology, Nanjing University, Nanjing 210093, People's Republic of China
[b] College of Plant Protection, Jiangsu Key Laboratory of Pesticide Science, Nanjing Agricultural University, Nanjing 210095, People's Republic of China

ARTICLE INFO

Article history:
Received 20 April 2011
Revised 13 June 2011
Accepted 15 June 2011
Available online 21 June 2011

Keywords:
Cinnamic acid
EGFR
Anilinoquinazoline
Antiproliferative

ABSTRACT

A novel type of cinnamic acid quinazoline amide derivatives (**20**–**42**), which designed the combination between quinazoline as the backbone and various substituted cinnamic acid as the side chain, have been synthesized and their biological activities were evaluated within cytotoxicity assay firstly and then potent EGFR inhibitory activity. Compound **42** demonstrated the most potent inhibitory activity (IC_{50} = 0.94 μM for EGFR), which could be optimized as a potential EGFR inhibitor in the further study. Docking simulation was performed to position compound **42** into the EGFR active site to determine the probable binding model. Analysis of the binding conformation of **42** in active site displayed compound **42** was stabilized by hydrogen bonding interactions with Lys822, which was different from other derivatives. In the further study, Compounds **43** and **44** had been synthesized and their biological activities were also evaluated, which were the same as that we expected. Compound **43** has demonstrated significant EGFR (IC_{50} = 0.12 μM) and tumor growth inhibitory activity as a potential anticancer agent.

1. Introduction

The altered protein expression and activity of receptor tyrosine kinases (TK) are implicated in the progression of various types of cancers. One such dysfunction is the overexpression of the epidermal growth factor receptor (EGFR) and its closest homologue HER2 (erbB2) that correlates with aggressive tumor progression and poor prognosis.[1] Unlike more standard chemotherapy agents, which destroy both cancer cells and healthy cells, EGFR inhibitor targeted cancer treatment primarily attach to and destroy cancer cells. Because of this, EGFR inhibitor therapies have fewer broad-range side effects such as the nausea and vomiting, hair loss, and anemia sometimes associated with more traditional chemotherapy. Selective inhibitors of tyrosine phosphorylation by EGFR have become an important class of potential anticancer drugs.[2–4] Several classes of inhibitors have been reported with the most potent and selective being the 4-(phenylamino)quinazolines.[5–8] Kinetic studies[6,9] show that these compounds selectively inhibit EGF-stimulated signal transduction by reversibly binding at the ATP site of EGFR. As we all know, three 4-(phenylamino)quinazolines, Gefitinib[10] (CP 358774), Erlotinib (ZD 1839)[11] and Lapatinib (GW572016)[12] have been approved by FDA in these years (Fig. 1).

Substituted cinnamic acids are widely distributed in the plant kingdom and are found in coffee beans, olives, propolis, fruits, and vegetables. They are found usually as simple derivatives including amide, esters, sugar esters, and glycosides.[13] Hydroxycinnamic acid esters are widely distributed in the plant kingdom and are reported as cellular antioxidants, anti-inflammatory agents, or inhibitors of enzymes involved in cell proliferation, and some biological activities.[14–16] Antitumor activities of various cinnamic acid derivatives were also explored by many research groups. Particularly, cinnamic acid ester derivatives showed the potential antitumor activity.[17–19] It was reported that compound **3h** demonstrated the most potent inhibitory activity (IC_{50} = 0.62 μM for EGFR and IC_{50} = 2.15 μM for HER-2), which was compared with the positive control Erlotinib.[20]

It is an increasing interest that combi-molecules are agents designed to block multiple targets in cancer cells due to complex formation mechanism of tumor. One common strategy is to make an ester or amide as a prodrug by the combination of two structural scaffold pointed to different target spot. Our initial modeling studies of the binding of reversible anilinoquinazoline suggested a binding mode whereby the 6- and 7-positions of the bicyclic chromophore point toward the solvent out of the ATP binding pocket. This explains why both positions can be used to add bulky solubilizing functionalities to inhibitors without losing binding affinity.[10,11,21,22] In this study, aminoquinazolines that binds to the ATP site of EGFR and cinnamic acid derivatives, which also have anti-cancer activity reported, would be assembled firstly and the latter have been

* Corresponding author. Tel./fax: +86 25 83592672.
E-mail address: zhuhl@nju.edu.cn (H.-L. Zhu).
† These authors contributed equally to this work.

0968-0896/$ - see front matter Crown Copyright © 2011 Published by Elsevier Ltd. All rights reserved.
doi:10.1016/j.bmc.2011.06.044

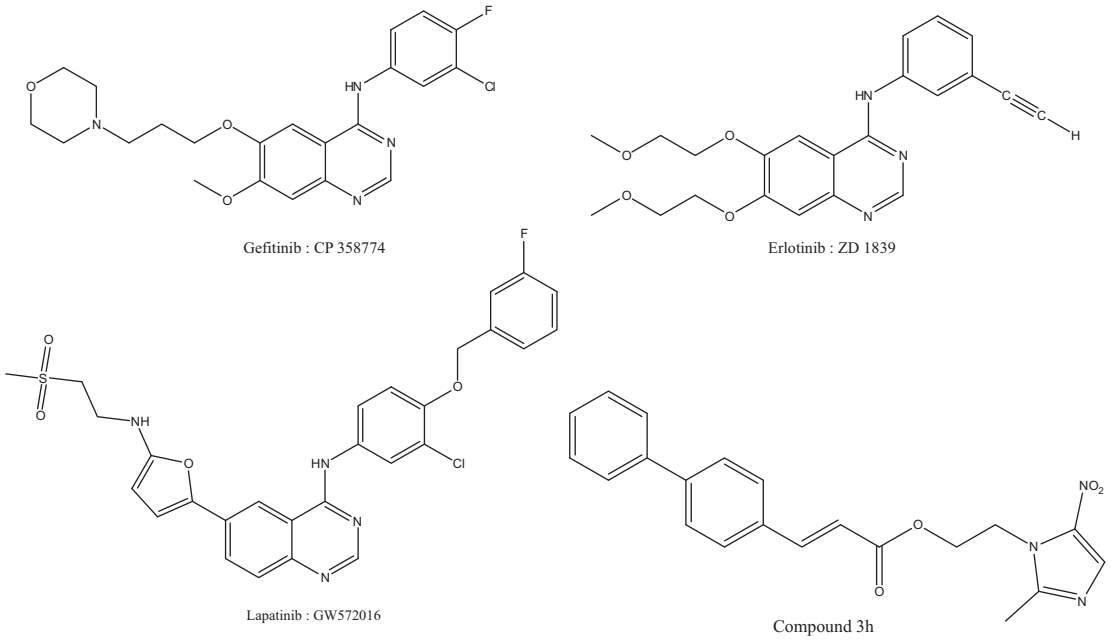

Figure 1. The structure of Gefitinib, Erlotinib, Lapatinib and compound **3h**.

grafted to the 6- and 7-positions of the bicyclic chromophore. The question whether these new molecules could keep significant EGFR inhibitory activity or just like combi-molecules might degrade two pharmacophores applied to different targets and get an exciting outcome, may be unclear. We postulates that a molecule termed 'combinatorial molecule' designed to interact with the epidermal growth factor receptor (EGFR) on its own and the activity of the two together would perform better. We described the synthesis and the SAR of the novel series of cinnamic acid quinazoline amide derivatives, and the biological activity evaluation indicated that some of these compounds are potent inhibitors of EGFR. Docking simulations were performed using the X-ray crystallographic structure of the EGFR in complex with an inhibitor to explore the binding modes of these compounds at the active site.

2. Results and discussion

2.1. Chemistry

The synthesis of compounds **5** and **6** proceeded in the same way according to Scheme 1, 2-amino-5-nitrobenzonitrile **1** was treated in commercially available dimethylformamide dimethyl acetal to give **2** (Scheme 1). Compound **2** was added in acetic acid containing 3-bromobenzenamine or 3-chlorobenzenamine to give **3** or **4**, respectively. Reduction of these nitro compounds with Fe gave the targeted amines **5** and **6** in the next step. In parallel, the substituted cinnamic acids **7–19** were synthesized according to Scheme 2 and these cinnamic acids were converted to acid chlorides before reacted with **5** or **6** in Scheme 3. Treatment of amine with acyl chloride from **7–19** in EtOAc at ice-bath gave the required amides (Table 1). The latter compounds were purified by column chromatography on silica gel with a mixture of ethyl acetate/petroleum ether as eluent. Compounds **43** and **44** were also synthesized according to Scheme 4 in the further study. All of the synthetic compounds gave satisfactory analytical and spectroscopic data, which were in full accordance with their depicted structures.

2.2. Biological activity

2.2.1. Antiproliferation assay

The structures of the quinazoline amides studied are listed in Table 1, together with their potencies for inhibition of A549 cells and F10 cells by applying the MTT colorimetric assay. Compounds were tested over a range of concentrations from 0.01 to 100 μg/ml, and the calculated IC_{50} values, that is, the concentration (μg/mL) of a compound that was able to cause 50% growth inhibition with respect to the control culture, were reported differently according to different cancer cells. Obviously, all the compounds remarked antiproliferative activities, and generally the results showed which those applied to F10 cells would performed better than that in A549 cells.

Anilinoquinazoline derivatives as a lead compound have been studying in these years and there were some empirical rules concluded: (1) the N1, N3 of quinazoline would interact with active center probably by hydrogen bond, water bridge or else. So we saved the quinazoline skeleton. (2) The *meta*-substituent of the aniline group is oriented toward the kinase pocket. This mode of binding is in line with the structure–activity relationship observed in the quinazoline inhibition series. Small substituents are tolerated at the 3′-aniline moiety, preferentially halogens and electron-donating group at the 6- and/or 7-positions that enhance the binding of N1 and N3. Although the aniline NH does not form an H-bond, its replacement with a methyl group is deleterious for activity.[23] In this study, we choose halogen atom (Br and Cl) at the 3'-aniline moiety and generally the former has greater potency than the latter in some research reported.[23] From **20–31** to **32–42**, there are no obvious difference between Br and Cl, **20** compared to **32**, **21** compared to **33**, and so on. The reason for this is probably due to the cinnamic acid structure. As for the compounds with one substituent on the cinnamic acid ring, we found a straightforward correlation between the electronic property and cytotoxicity, generally the more electron-donating group at the R_3 position would increase the cytotoxicity except **31** and **42**. This was supported by two groups (compounds **22**, **24**, **26**, and compounds **34**, **36**). Also there might be other effects at the R_3 position.

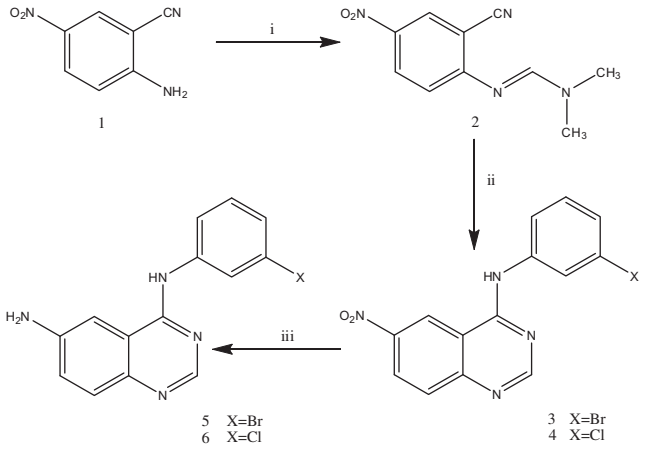

Scheme 1. Synthesis of quinazolines **5** and **6**. Reagents and conditions: (i) dimethylformamide dimethyl acetal, 70–75 °C; (ii) $ArNH_2$/AcOH, 70–75 °C; (iii) Fe/AcOH/EtOH/H_2O, 70–80 °C.

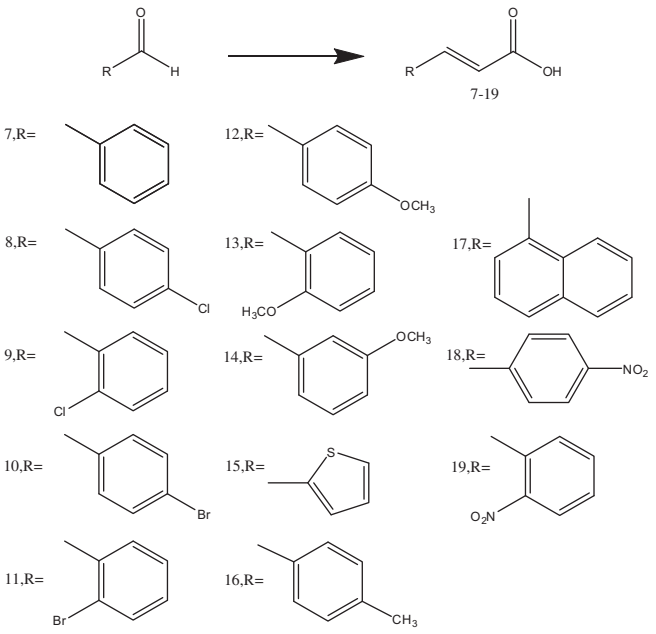

Scheme 2. Synthesis of cinnamic acid derivatives **7**–**19**. Reagents and conditions: $HOOCCH_2COOH$/pyridine/piperidine, 80 °C, 24 h/reflux.

We guessed the conjugated effect from halogen interacting with double bond would make great contribution for electron-donation and steric effect should not be ignored. The reason why **26** was weaker than **24** might be the size of methoxyl group.

We still premised that the interactions of the molecule was the ATP binding site of EGFR, which quinazoline ring was buried inside the pocket and the substituent at the 6- and/or 7-positions was outside the cleft. Against human cancer cell lines, compounds **23** and **33** were approximately less10-fold active than **21** and **35**, respectively. This result indicated that replacement of the R_1 position by a same halogen group with substituent on aniline was beyond the field of electronic effect. The explanation might be that these two compounds with low bioactivity could not insert in the ATP cleft of EGFR and this would be put into further study. It was a bold surmise that the same group at the R_1 and R_4 position had great effect on the conformation of quinazoline ring. Obviously the electron-donating group at the R_1 position would keep the cytotoxicity, referring to **25** with OCH_3 and **29** with CH_3.

Structure–activity relationships in these derivatives demonstrated that compounds with substitution at the *meta* (**27**)- or *ortho* (**26**, **31**, **42**)-position showed more potent activities than those with substitution at the *para*-position (**25**, **30**, **41**) and a comparison of **27**, **26**, **25** based both on cytotoxicity and enzyme inhibitory activity demonstrated that the potency order of the same group besides Br and Cl was *para* < *ortho* < *meta*. We could speculate that the *meta* NO_2 compound would be superior to **30**, **31** or **41**, **42**. Meanwhile, we also could conclude that benzene ring as a framework performed better than thiazole ring and similarly as naphthalene ring from **20** comparing **28**, and **32** comparing **38**, **40**.

2.2.2. Enzyme assay

To evaluate the EGFR inhibitory potency of new compounds, their ability to block EGFR TK was tested in an EGFR TK assay. We chose the twelve compounds behaved well for antiproliferation and their activities positively correlated with antiproliferative activity, which they had the same trends (Table 2). This could indicate that cinnamic acid anilinoquinazoline derivatives basically follow the EGFR inhibition path against cancer cell. Overall the bulky moiety of the 6-position of each quinazoline was not deleterious for activity. As shown in Table 2, compound **31** and **42** displayed the most potent inhibitory activity (IC_{50} = 1.02 and 0.94 μM for EGFR), less comparable to the positive control Erlotinib (IC_{50} = 0.03 μM for EGFR).

So as to gain more understanding of the structure–activity relationships observed at the EGFR, molecular docking of the most potent inhibitor **42** into ATP binding site of EGFR kinase was performed on the binding model based on the EGFR complex structure (1M17.pdb). The binding model of compound **42** and EGFR was depicted in Figures 2A and 2B. In the binding model, compound **42**′ quinazoline ring be inserted nicely inside the pocket, and outside the cleft, and the oxygen atom of nitro group of **42** also forms hydrogen bond with the amino hydrogen of Lys822, which made the combination ability of **42** acting on EGFR. This was likely the explanation for why nitro-group was not electron-donating group but had good outcome. Meanwhile, we chose **32** without any substituent on the cinnamylate ring as the positive control in the docking procedure (Fig. 3). It was expected that there was no apparent hydrogen bond outside the cleft and for the interaction between compounds and EGFR the nitro counted for much. The enzyme assay data and the molecular docking results showed that compound **42** was a potential inhibitor of EGFR (Fig. 2).

Compounds **21**, **31**, **40**, **42**, which had small differences on integrating with EGFR and potent inhibitory activity showed high antiproliferative activity against cancer cells with IC_{50} ranging from 0.3 to 0.671 μg/mL, which indicated that these cinnamic acid quinazoline amide derivatives were potent inhibitor of EGFR as antitumor agents. Among these compounds, compound **42** exhibited the most potential inhibitory activity in tumor growth inhibition and exhibited favored EGFR inhibitory activity. Meanwhile we could go into the further study in which we could save the *meta*-nitro and increase electron donation of the side chain.

2.2.3. Further study

In order to get the expectation above, Compound **43** and **44** have been synthesized and their biological activities shown in Table 3 were also evaluated. We would choose the compounds containing nitro group to test their cytotoxicity using the A431 cell, which over expresses EGFR, and EGFR inhibitory activity correspondingly. As we expected, compound **43** and **44** containing *meta*-nitro group performed better than other derivatives, which displayed the most potent inhibitory activity (IC_{50} = 0.12 and 0.19 μM for EGFR), com-

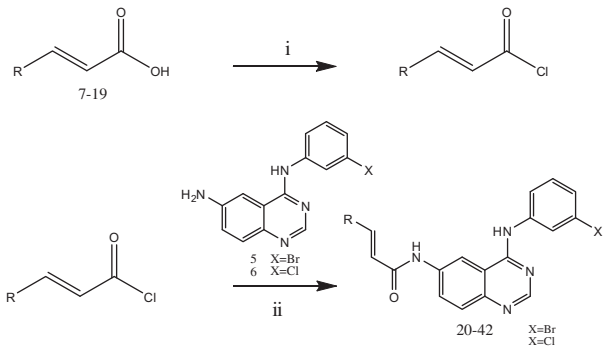

Scheme 3. Synthesis of cinnamic amide derivatives **20**–**42**. Reagents and conditions: (i) $SOCl_2$, 70–80 °C, reflux, 4 h; (ii) EtOAC/K_2CO_3, ice-bath, reflux, overnight.

parable to the positive control Erlotinib (IC_{50} = 0.03 μM for EGFR). The fact that the *meta* NO_2 compounds are superior to **30**, **31** or **41**, **42** is acceptable. As for the binding mode of the *meta* NO_2 compounds, we had gotten molecular docking of compound **43** into the three-dimensional EGFR complex structure (1M17.pdb) using the autodock software package and this showed **43** had possessed the same binding mode as **42** and the cinnamylate ring looked like more relaxed than the latter (Fig. 4). In the comparison to Erlotinib's binding mode, the formation of hydrogen bond with Lys822 seemed significance for **43** and the binding_energy was up to −13.73, better than −8.83 from the optimal binding conformation of Erlotinib. Among these compounds, compound **43** would share the same binding mode with other NO_2 compounds and exhibited the most potential inhibitory activity both in tumor growth inhibition and EGFR inhibitory activity.

3. Conclusions

A series of cinnamic acid quinazoline amide derivatives have been designed and synthesized, and their biological activities were also evaluated as cytotoxicity assay firstly and then potent EGFR inhibitory. Compound **42** demonstrated the most potent inhibitory activity (IC_{50} = 0.94 μM for EGFR), which could be optimized as a potential EGFR inhibitor in the further study. Docking simulation was performed to position compound **42** into the EGFR active site to determine the probable binding model. Analysis of the binding conformation of **42** in active site displayed the compound **42**′ cinnamylate side chain was stabilized by hydrogen bonding interactions with Lys822, which was different from other derivatives. Antiproliferative assay results also showed that these cinnamic acid quinazoline amide derivatives had the potential to be developed for antiproliferative agents against cancer cells. Based on this, compounds **43** and **44** were obtained according to Scheme 4 in the next step and we also gave the relevant bioactivity evaluation to these compounds. Among these compounds, we could conclude that compound **43** has demonstrated significant EGFR (IC_{50} = 0.12 μM) and tumor growth inhibitory activity as a potential anticancer agent.

4. Experiments

4.1. Materials and methods

^{1}H NMR spectra were measured on a Bruker AV-300 or AV-500 spectrometer at 25 °C and referenced to Me_4Si. Chemical shifts are reported in ppm (δ) using the residual solvent line as internal standard. Splitting patterns are designed as s, singlet; d, doublet; t, triplet; m, multiplet. ESI-MS spectra were recorded on a Mariner System 5304 Mass spectrometer. Elemental analyses were performed on a CHN-O-Rapid instrument and were within ±0.4% of the theoretical values. Melting points were determined on a XT4 MP apparatus (Taike Corp., Beijing, China) and are as read. Analytical thin-layer chromatography (TLC) was performed on the glass-backed silica gel sheets (silica gel 60 Å GF254). All compounds were detected using UV light (254 or 365 nm).

4.2. General procedure for the preparation of compounds 5, 6 (Scheme 1)

*N*4-(3-Bromophenyl)quinazoline-4,6-diamine (**5**) or *N*4-(3-chlorophenyl)quinazoline-4,6-diamine (**6**) was prepared according to the literature procedure.[24] 5-Nitroanthranilonitrile **1** (4.89 g, 30 mmol, 1.0 equiv) was suspended in dimethylformamide dimethyl acetal (10 mL) and the mixture was refluxed for 2 h. The resulting mixture was cooled to room temperature for 2–3 h. The yellow precipitate that formed was filtered, washed with ethyl ether, and dried to give **2** (yield: 80–90%). A mixture of **2** (2.18 g, 10 mmol, 1.0 equiv) and 3-chloroaniline (1.1 equiv) or 3-bromoaniline (1.1 equiv) were heated and stirred at reflux in acetic acid (20 mL) for 2 h. Aniline and acetic acid would be added into the reaction flask first and then slowly added **2** using the medicine spoon within one minute. This treatment is to prevent the formation of lumps between them. The yellow precipitate that formed was filtered hot, washed with hot acetic acid, diethyl ether, and dried to give the desired nitroquinazoline **3** or **4** (yield: 80–90%).

6-Nitroquinazoline **4** (2.0 g, 6.65 mmol, 1.0 equiv), iron (2.5 g, 45 mmol, 6.7 equiv) and acetic acid (6 mL, 90 mmol, 13.5 equiv) were suspended in aqueous ethanol (180 mL, 77.8% v/v) and heated at reflux about 70–80 °C for 5–6 h. Meantime this mixture would be stirred for one minute every half hour with a glass rod and the yellow solution would become reddish-brown slowly. The reaction mixture was cooled to room temperature and alkalinized by addition of concentrated ammonia (40 mL). Insoluble material was removed by filtration through Celite, and the filtrate was evaporated under reduced pressure. The resulting solid was extracted with ethyl acetate for column chromatography. Column chromatography was performed using silica gel (200–300 mesh) eluting with ethyl acetate and petroleum ether (3:1, v/v) to give amine **6** (Yield: 50–60%). Mp 163–164 °C; ^{1}H NMR (300 MHz, DMSO-d_6, δ ppm): 4.08 (s, 2H, NH_2), 6.93 (s, 1H), 7.13 (d, J = 7.86, 2H), 7.24 (dd, J_1 = 11.13 Hz, J_2 = 8.97 Hz, 1H), 7.33 (t, J = 8.06 Hz, 1H), 7.59 (d, J = 7.68 Hz, 1H), 7.78 (d, J = 8.97 Hz,1H), 7.94 (s,1H), 8.65 (s, 1H, NH). ESI-MS: 271.1 ($C_{14}H_{11}ClN_4$, $[M+H]^+$). Anal. Calcd for $C_{14}H_{10}ClN_4$: C, 62.11; H, 4.10; N, 20.70. Found: C, 61.93; H, 4.36; N, 21.07. It is surprising that the ^{1}H NMR data obtained was inconsistent with the results reported in the literature.[24]

*N*4-(3-Bromophenyl)quinazoline-4,6-diamine (**5**) was also prepared as described for **6**.

4.3. Preparation of substituted cinnamic acids 7–19 (Scheme 2)

The substituted cinnamic acids were synthesized using Doebner Knoevenagel modification.[25] Cinnamic acids were prepared by mixing substituted benzaldehydes (3.2 mM), malonic acid (3.87 mM), pyridine (20 mL), and piperidine (40 μL) together and stirring 80 °C on a magnetic stirrer for 24 h (Scheme 2). The reaction mixture was evaporated under reduced pressure. Precipitates obtained were filtered, washed with cold water repeatedly, and dried. Finally the mixtures were recrystallized with dichloromethane to give these acids (Trans-isomer). The yields were between 70% and 80%. Two compounds (**13**, **16**) due to intermediate products were randomly selected to give the determination of structure.

4.3.1. (*E*)-3-(2-Methoxyphenyl)acrylic acid (13)

Mp 184–186 °C; ^{1}H NMR (500 MHz, DMSO-d_6, δ ppm): 3.87 (s, 3H, OCH_3), 6.51 (d, J = 16.2 Hz, 1H), 6.98 (t, J = 7.47 Hz, 1H), 7.09

Table 1
Structure of cinnamic acid quinazoline amide derivatives and the antiproliferative effect

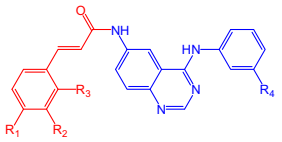

Compound	R_1	R_2	R_3	R_4	IC_{50} (μg/mL)	
					Growth inhibition in A549 cells[a]	Inhibition of serum-stimulated growth in F10 cells[a]
20	H	H	H	Br	3.96	1.45
21	Cl	H	H	Br	1.06	0.38
22	H	H	Cl	Br	6.63	2
23	Br	H	H	Br	15.32	10.65
24	H	H	Br	Br	2.38	0.92
25	OCH_3	H	H	Br	3.36	1.24
26	H	H	OCH_3	Br	3.55	1.28
27	H	OCH_3	H	Br	2.05	0.87
28	—	—	—	Br	4.66	2.51
29	CH_3	H	H	Br	3.01	1.39
30	NO_2	H	H	Br	1.85	0.9815
31	H	H	NO_2	Br	0.92	0.338
32	H	H	H	Cl	1.58	0.68
33	Cl	H	H	Cl	12.43	9.97
34	H	H	Cl	Cl	4.58	1.74
35	Br	H	H	Cl	1.86	0.75
36	H	H	Br	Cl	5.63	1.65
37	H	OCH_3	H	Cl	2.58	1.05
38	—	—	—	Cl	9.23	4.26
39	CH_3	H	H	Cl	6.03	2.02
40	—	—	—	Cl	1.49	0.671
41	NO_2	H	H	Cl	5.26	2.05
42	H	H	NO_2	Cl	0.78	0.3
Erlotinib	—	—	—	—	0.13	0.02

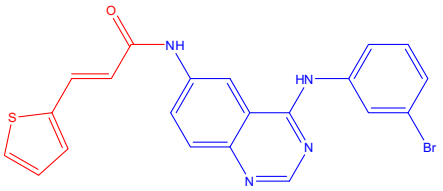

28

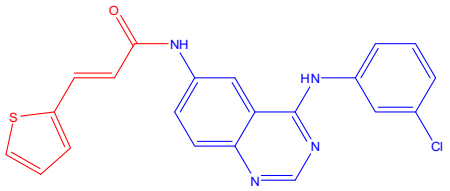

38

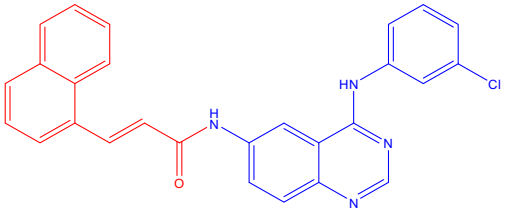

40

[a] Cell growth was measured using the MTT assay. Values are the average of two independent experiments run in triplicate. Variation was generally 1%.

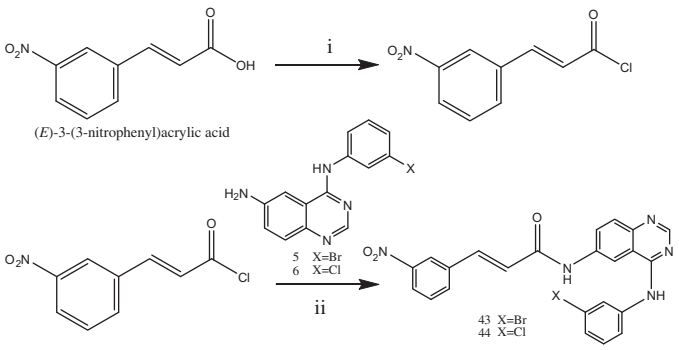

Scheme 4. Synthesis of cinnamic amide derivatives **43** and **44**. Reagents and conditions: (i) $SOCl_2$, 70–80 °C, reflux, 4 h; (ii) EtOAC/K_2CO_3, ice-bath, reflux, overnight.

Table 2
Inhibition (IC_{50}) of EGFR kinase

Compound	EGFR inhibition IC_{50} (μM)
21	1.21
24	4.28
25	7.22
26	7.71
27	6.02
30	5.16
31	1.02
32	3.61
35	3.49
37	6.63
40	2.81
42	0.94
Erlotinib	0.03

(d, J = 8.1 Hz, 1H), 7.39–7.42 (m, 1H), 7.67 (dd, J_1 = 7.8 Hz, J_2 = 7.6 Hz, 1H), 7.83 (d, J = 16.2 Hz, 1H), 12.27 (s, 1H, COOH). ESI-MS: 179.1 ($C_{10}H_{10}O_3$, $[M+H]^+$). Anal. Calcd for $C_{10}H_9O_3$: C, 67.41; H, 5.66. Found: C, 67.99; H, 5.36.

4.3.2. (*E*)-3-*p*-Tolylacrylic acid (16)

Mp 198–200 °C; ^{1}H NMR (300 MHz, DMSO-d_6, δ ppm): 2.33 (s, 3H, CH_3), 6.46 (d, J = 16.11 Hz, 1H), 7.55 (t, J = 8.31 Hz, 3H), 7.23 (d, J = 7.86 Hz, 1H), 12.33 (s, 1H, COOH). ESI-MS: 163.1 ($C_{10}H_{10}O_2$, $[M+H]^+$). Anal. Calcd for $C_{10}H_9O_2$: C, 74.06; H, 6.21. Found: C, 74.23; H, 5.96.

4.4. General synthesis method of substituted cinnamic acid amide analogues 20–42 (Scheme 3)

The starting materials (acids **7–19**) for the synthesis of amides should be activated in the first procedure: the compounds **7–19** (1.0 mM) and $SOCl_2$ (6–10 mL) were mixed and stirred at reflux 80°Cfor 4 h. The reaction mixture was cooled and evaporated to give reactive acyl chloride obtained as an oil, which would be dissolved in ethyl acetate (5–6 mL) in the next step.

A solution of acyl chloride (1.0 mM) in ethyl acetate was added dropwise to compounds **5** or **6** (0.5 mM) in ethyl acetate containing potassium carbonate (600 mg) at 0 °C with constant stirring overnight. The reaction mixture was then poured in excess of diluted NaOH and extracted with EtOAc .The extraction liquid was purified by a flash chromatography with EtOAc/petroleum ether (3:1, v/v) to give these cinnamamides as follows: the yields were between 40% and 60%.

4.4.1. (*E*)-*N*-(4-(3-Bromophenylamino)quinazolin-6-yl)cinnamamide (20)

Compound **20** was prepared as described above. Mp 265–266 °C; ^{1}H NMR (300 MHz, DMSO-d_6, δ ppm): 6.92 (d, J = 15.72 Hz, 1H), 7.27–7.37 (m, 2H), 7.42–7.48 (m, 3H), 7.66 (t, J = 7.7 Hz, 3H), 7.79–7.87 (m, 2H), 7.94 (dd, J_1 = 8.97 Hz, J_2 = 8.97 Hz, 1H), 8.17 (s, 1H, NH), 8.59 (s, 1H), 8.83 (s, 1H), 9.97 (s, 1H), 10.55 (s, 1H, NHCO). ESI-MS: 445.1 ($C_{23}H_{17}BrN_4O$, $[M+H]^+$). Anal. Calcd for $C_{23}H_{16}BrN_4O$: C, 62.03; H, 3.85; N, 12.58. Found: C, 61.99; H, 4.16; N, 13.01.

4.4.2. (*E*)-*N*-(4-(3-Bromophenylamino)quinazolin-6-yl)-3-(4-chlorophenyl)acrylamide (21)

Mp 283–285 °C; ^{1}H NMR (300 MHz, DMSO-d_6, δ ppm): 6.93 (d, J = 15.7 Hz, 1H), 7.3 (d, J = 7.95 Hz, 1H), 7.35 (t, J = 8.02 Hz, 1H), 7.54 (d, J = 8.55 Hz, 2H), 7.65–7.70 (m, 3H), 7.82 (d, J = 8.85 Hz, 1H), 7.88 (d, J = 8.1 Hz, 1H), 7.96 (dd, J_1 = 9 Hz, J_2 = 8.85 Hz, 1H), 8.19 (s, 1H, NH), 8.6 (s, 1H), 8.83 (s, 1H), 9.95 (s, 1H, OH), 10.56 (s, 1H, NHCO). ESI-MS: 479.0 ($C_{23}H_{16}BrClN_4O$, $[M+H]^+$). Anal. Calcd for $C_{23}H_{15}BrClN_4O$: C, 57.58; H, 3.36; N, 11.68. Found: C, 57.87; H, 3.12; N, 11.57.

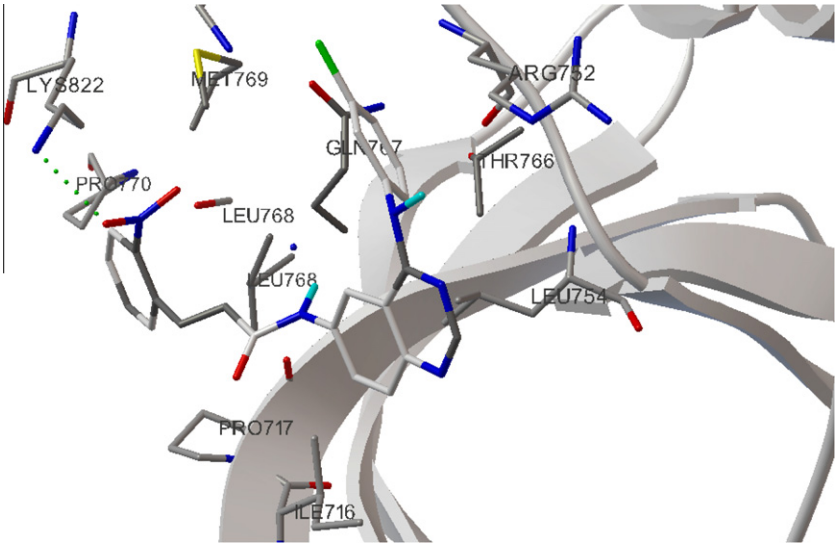

Figure 2A. Docking of compound **42** interacting with EGFR kinase (1M17.pdb) shows intermolecular hydrogen bond between Lys822 and O from NO_2.

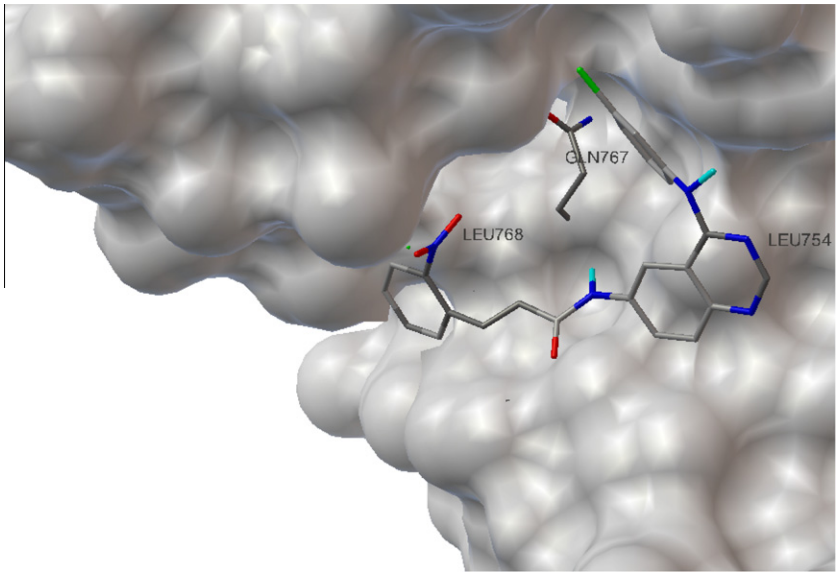

Figure 2B. 3D model of the interaction between compound **42** and the ATP binding site. The cinnamic acid chain anchors outside the site, and the nitro group could form hydrogen bond to stabilize the combination, which binding energy is equal to −12.15.

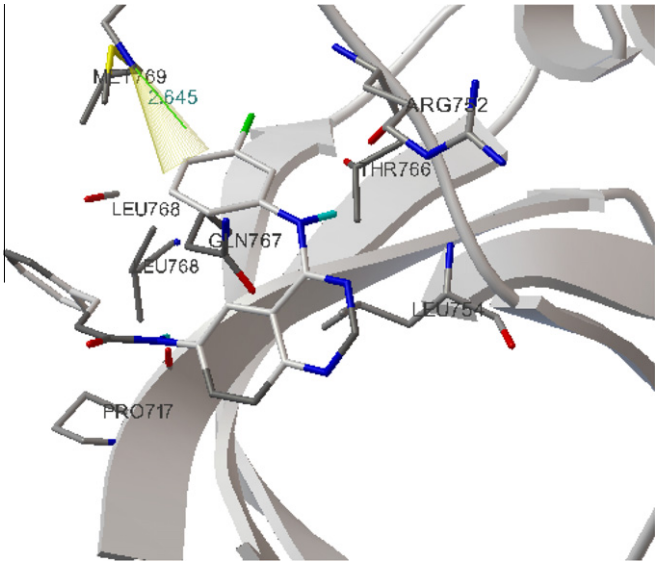

Figure 3A. Docking of compound **32** interacting with EGFR kinase (1M17.pdb) shows there is no other interaction between cinnamic acid side chain and EGFR except pi-cation interaction inside the pocket.

4.4.3. (*E*)-*N*-(4-(3-Bromophenylamino)quinazolin-6-yl)-3-(2-chlorophenyl)acrylamide (22)

Mp 287–288 °C; ^{1}H NMR (300 MHz, DMSO-d_6, δ ppm): 6.97 (d, J = 15.54 Hz, 1H), 7.27–7.37 (m, 2H), 7.44–7.47 (m, 2H), 7.59 (t, J = 4.67 Hz, 1H), 7.79–8.00 (m, 5H), 8.17 (s, 1H, NH), 8.59 (s, 1H), 8.88 (s, 1H), 9.97 (s, 1H), 10.66 (s, 1H, NHCO). ESI-MS: 479.0 ($C_{23}H_{16}BrClN_4O$, $[M+H]^+$). Anal. Calcd for $C_{23}H_{15}BrClN_4O$: C, 57.58; H, 3.08; N, 10.69. Found: C, 58.03; H, 3.36; N, 9.87.

4.4.4. (*E*)-*N*-(4-(3-Bromophenylamino)quinazolin-6-yl)-3-(4-bromophenyl)acrylamide (23)

Mp 295–296 °C; ^{1}H NMR (300 MHz, DMSO-d_6, δ ppm): 6.95 (d, J = 15.72 Hz, 1H), 7.29–7.39 (m, 2H), 7.61–7.75 (m, 5H), 7.84 (t, J = 10.52 Hz, 2H), 7.96 (d, J = 8.94 Hz, 1H), 8.18 (s, 1H, NH), 8.6 (s, 1H), 8.84 (s, 1H), 10 (s, 1H), 10.59 (s, 1H, NHCO). ESI-MS: 523.0 ($C_{23}H_{16}Br_2N_4O$, $[M+H]^+$). Anal. Calcd for $C_{23}H_{15}Br_2N_4O$: C, 52.70; H, 3.08; N, 10.69. Found: C, 52.43; H, 3.36; N, 10.89.

4.4.5. (*E*)-*N*-(4-(3-Bromophenylamino)quinazolin-6-yl)-3-(2-bromophenyl)acrylamide (24)

Mp 293–294 °C; ^{1}H NMR (300 MHz, DMSO-d_6, δ ppm): 6.94 (d, J = 15.54 Hz, 1H), 7.37 (t, J = 8.69 Hz, 3H), 7.52 (t, J = 7.5 Hz, 1H), 7.74–7.85 (m, 4H), 7.96 (t, J = 7.86 Hz, 2H), 8.16 (s, 1H, NH), 8.64 (s, 1H), 8.95 (s, 1H), 10.16 (br s, 1H), 10.72 (s, 1H, NHCO). ESI-MS: 523.0 ($C_{23}H_{16}Br_2N_4O$, $[M+H]^+$). Anal. Calcd for $C_{23}H_{15}Br_2N_4O$: C, 52.70; H, 3.08; N, 10.69. Found: C, 52.83; H, 3.23; N, 10.33.

4.4.6. (*E*)-*N*-(4-(3-Bromophenylamino)quinazolin-6-yl)-3-(4-methoxyphenyl)acrylamide (25)

Mp 239–240 °C; ^{1}H NMR (300 MHz, DMSO-d_6, δ ppm): 3.83 (s, 3H, OCH_3), 7.02–7.10 (m, 2H), 7.29–7.39 (m, 2H), 7.63 (t, J = 7.49 Hz, 1H), 7.82–7.94 (m, 5H), 8.03 (dd, J_1 = 8.97 Hz, J_2 = 8.97 Hz, 1H), 8.2 (s, 1H, NH), 8.63 (s, 1H), 8.79 (s, 1H), 9.98 (s, 1H), 10.51 (s, 1H, NHCO). ESI-MS: 475.0 ($C_{24}H_{19}BrN_4O_2$, $[M+H]^+$). Anal. Calcd for $C_{24}H_{18}BrN_4O_2$: C, 60.64; H, 4.03; N, 11.79. Found: C, 60.85; H, 4.23; N, 11.43.

4.4.7. (*E*)-*N*-(4-(3-Bromophenylamino)quinazolin-6-yl)-3-(2-methoxyphenyl)acrylamide (26)

Mp 307–308 °C; ^{1}H NMR (300 MHz, DMSO-d_6, δ ppm): 3.89 (s, 3H, OCH_3), 6.93–7.05 (m, 2H), 7.11 (d, J = 8.04 Hz, 1H), 7.28–7.38 (m, 2H), 7.42 (d, J = 7.14 Hz, 1H), 7.59 (d, J = 7.68 Hz, 1H), 7.79–7.86 (m, 3H), 7.91–7.96 (m, 1H), 8.16 (s, 1H, NH), 8.6 (s, 1H), 8.85 (s, 1H), 10.01 (br s, 1H), 10.54 (s, 1H, NHCO). ESI-MS: 475.0 ($C_{24}H_{19}BrN_4O_2$, $[M+H]^+$). Anal. Calcd for $C_{24}H_{18}BrN_4O_2$: C, 60.64; H, 4.03; N, 11.79. Found: C, 60.94; H, 4.31; N, 11.40.

4.4.8. (*E*)-*N*-(4-(3-Bromophenylamino)quinazolin-6-yl)-3-(3-methoxyphenyl)acrylamide (27)

Mp 303–305 °C; ^{1}H NMR (300 MHz, DMSO-d_6, δ ppm): 3.83 (s, 3H, OCH_3), 6.88–7.07 (m, 2H), 7.20–7.37 (m, 4H), 7.47 (d, J = 8.79 Hz, 1H), 7.80–7.93 (m, 4H), 8.17 (s, 1H, NH), 8.58 (s, 1H), 8.9 (s, 1H), 9.94 (br s, 1H), 10.64 (s, 1H, NHCO). ESI-MS: 475.0

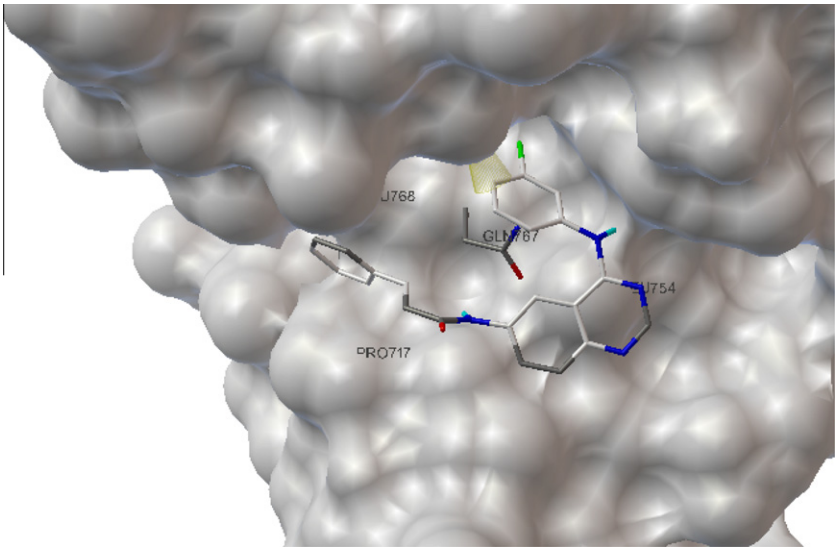

Figure 3B. 3D model of the interaction between compound **32** and the ATP binding site.

Table 3
EGFR tyrosine kinase (TK) inhibition and antiproliferative data for combinatorial molecules containing nitro group

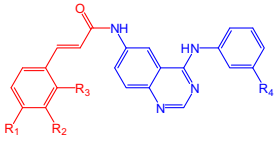

Compound	R_1	R_2	R_3	R_4	IC_{50} (μM)	
					EGFR enzyme assay	inhibition of A431 basal growth
5	—	—	—	Br	0.04	42
6	—	—	—	Cl	0.2	47
30	NO_2	H	H	Br	5.16	1.34
31	H	H	NO_2	Br	1.02	0.98
41	NO_2	H	H	Cl	3.45	2.13
42	H	H	NO_2	Cl	0.94	0.75
43	H	NO_2	H	Br	0.12	0.33
44	H	NO_2	H	Cl	0.19	0.49
Erlotinib	—	—	—	—	0.03	0.27

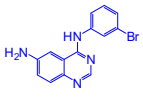

5

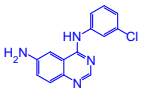

6

($C_{24}H_{19}BrN_4O_2$, $[M+H]^+$). Anal. Calcd for $C_{24}H_{18}BrN_4O_2$: C, 60.64; H, 4.03; N, 11.79. Found: C, 60.34; H, 3.98; N, 11.66.

4.4.9. (*E*)-*N*-(4-(3-Bromophenylamino)quinazolin-6-yl)-3-(thiophen-2-yl)acrylamide (28)

Mp 244 -246 °C; ^{1}H NMR (300 MHz, DMSO-d_6, δ ppm): 7.28 (dd, J_1 = 5.13 Hz, J_2 = 5.13 Hz, 1H), 7.33 (d, J = 4.59 Hz, 1H), 7.38 (d, J = 7.86 Hz, 1H), 7.76 (d, J = 2.91 Hz, 1H), 7.86 (t, J = 7.88 Hz, 2H), 7.95 (d, J = 5.1 Hz, 1H), 8.04 (dd, J_1 = 8.97 Hz, J_2 = 8.97 Hz, 1H), 7.74–7.85 (m, 4H), 7.96 (t, J = 7.86 Hz, 2H), 8.19 (s, 1H, NH), 8.32 (s, 1H), 8.64 (s, 1H), 8.79 (s, 1H), 10.04 (br s, 1H), 10.54 (s, 1H, NHCO). ESI-MS: 451.0 ($C_{21}H_{15}BrN_4OS$, $[M+H]^+$). Anal. Calcd for $C_{21}H_{14}BrN_4OS$: C, 55.88; H, 3.35; N, 12.41. Found: C, 55.83; H, 3.24; N, 12.63.

4.4.10. (*E*)-*N*-(4-(3-Bromophenylamino)quinazolin-6-yl)-3-p-tolylacrylamide (29)

Mp 248–249 °C; ^{1}H NMR (300 MHz, DMSO-d_6, δ ppm): 2.37 (s, 3H, CH_3), 7.32–7.39 (m, 5H), 7.81–7.85 (m, 3H), 7.9 (d, J = 7.86 Hz, 2H), 8.02 (d, J = 10.98 Hz, 1H), 8.21 (s, 1H, NH), 8.63 (s, 1H), 8.79 (s, 1H), 9.93 (s, 1H), 10.57 (s, 1H, NHCO). ESI-MS: 459.0 ($C_{24}H_{19}BrN_4O$, $[M+H]^+$). Anal. Calcd for $C_{24}H_{18}BrN_4O$: C, 62.75; H, 4.17; N, 12.20. Found: C, 63.03; H, 4.17; N, 11.83.

4.4.11. (*E*)-*N*-(4-(3-Bromophenylamino)quinazolin-6-yl)-3-(4-nitrophenyl)acrylamide (30)

Mp 300–302 °C; ^{1}H NMR (300 MHz, DMSO-d_6, δ ppm): 7.11 (d, J = 15.93 Hz, 1H), 7.29–7.39 (m, 2H), 7.75–7.99 (m, 6H), 8.18 (s, 1H, NH), 8.32 (d, J = 8.79 Hz, 2H), 8.61 (s, 1H), 8.85 (s, 1H), 10 (s, 1H), 10.71 (s, 1H, NHCO). ESI-MS: 490.0 ($C_{23}H_{16}BrN_5O_3$, $[M+H]^+$). Anal. Calcd for $C_{23}H_{15}BrN_5O_3$: C, 56.34; H, 3.29; N, 14.28. Found: C, 56.44; H, 3.38; N, 14.11.

4.4.12. (*E*)-*N*-(4-(3-Bromophenylamino)quinazolin-6-yl)-3-(2-nitrophenyl)acrylamide (31)

Mp 282–284 °C; ^{1}H NMR (300 MHz, DMSO-d_6, δ ppm): 6.9 (d, J = 15.54 Hz, 1H), 7.28–7.38 (m, 2H), 7.67–7.72 (m, 1H),

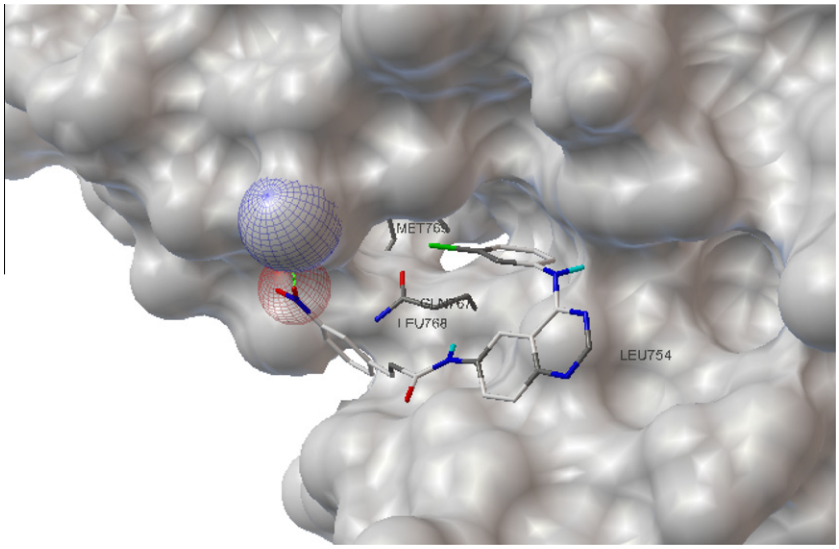

Figure 4A. 3D model of the interaction between compound **43** and the ATP binding site. The cinnamic acid chain anchors outside the site, and the nitro group could form hydrogen bond to stabilize the combination, which binding energy is equal to −13.33.

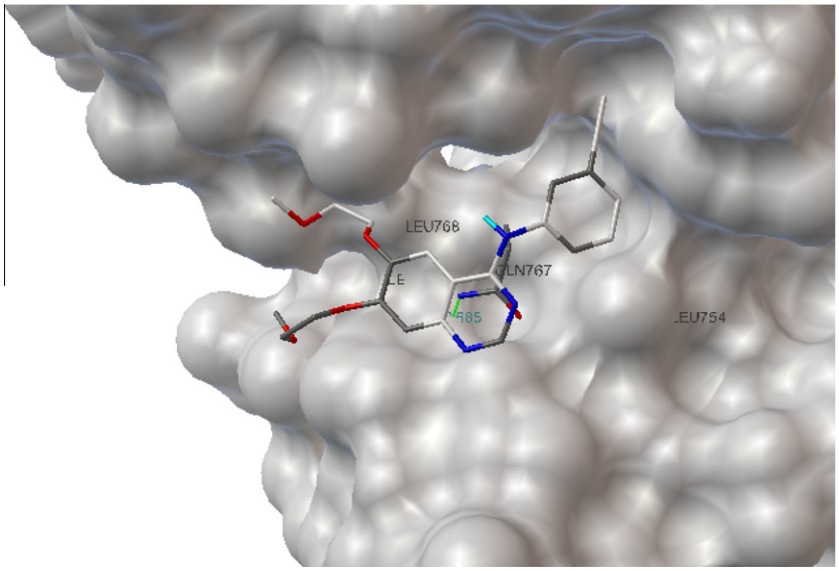

Figure 4B. The optimal model of the interaction between Erlotinib and the ATP binding site, which binding energy is equal to −8.83.

7.82–8.00 (m, 6H), 8.11 (d, J = 7.86 Hz, 1H), 8.18 (s, 1H, NH), 8.6 (s, 1H), 8.9 (s, 1H), 9.99 (s, 1H), 10.7 (s, 1H, NHCO). ESI-MS: 490.0 ($C_{23}H_{16}BrN_5O_3$, $[M+H]^+$). Anal. Calcd for $C_{23}H_{15}BrN_5O_3$: C, 56.34; H, 3.29; N, 14.28. Found: C, 56.22; H, 3.18; N, 14.53.

4.4.13. (*E*)-*N*-(4-(3-Chlorophenylamino)quinazolin-6-yl)cinnamamide (32)

Mp 294–295 °C; ^{1}H NMR (500 MHz, DMSO-d_6, δ ppm): 6.93 (d, J = 15.75 Hz, 1H), 7.16 (d, J = 7.8 Hz, 1H), 7.40–7.49 (m, 4H), 7.67 (t, J = 8.1 Hz, 3H), 7.82 (d, J = 8.65 Hz, 2H), 7.96 (d, J = 9 Hz, 1H), 8.07 (s, 1H, NH), 8.6 (s, 1H), 8.84 (s, 1H), 9.96 (s, 1H), 10.55 (s, 1H, NHCO). ESI-MS: 401.1 ($C_{23}H_{17}ClN_4O$, $[M+H]^+$). Anal. Calcd for $C_{23}H_{16}ClN_4O$: C, 68.91; H, 4.27; N, 13.98. Found: C, 68.99; H, 4.16; N, 13.91.

4.4.14. (*E*)-*N*-(4-(3-Chlorophenylamino)quinazolin-6-yl)-3-(4-chlorophenyl)acrylamide (33)

Mp 306–307 °C; ^{1}H NMR (500 MHz, DMSO-d_6, δ ppm): 6.93 (d, J = 15.75 Hz, 1H), 7.17 (d, J = 8.1 Hz, 1H), 7.17 (d, J = 8.1 Hz, 1H), 7.42 (t, J = 8.07 Hz, 1H), 7.54 (d, J = 8.4 Hz, 2H), 7.83 (d, J = 8.4 Hz, 2H), 7.65–7.70 (m, 3H), 7.97 (dd, J_1 = 9 Hz, J_2 = 9 Hz, 1H), 8.06 (s, 1H, NH), 8.6 (s, 1H), 8.83 (s, 1H), 9.99 (s, 1H, OH), 10.57 (s, 1H, NHCO). ESI-MS: 435.1 ($C_{23}H_{16}Cl_2N_4O$, $[M+H]^+$). Anal. Calcd for $C_{23}H_{15}Cl_2N_4O$: C, 63.46; H, 3.70; N, 12.87. Found: C, 63.05; H, 3.93; N, 13.01.

4.4.15. (*E*)-*N*-(4-(3-Chlorophenylamino)quinazolin-6-yl)-3-(2-chlorophenyl)acrylamide (34)

Mp 292–294 °C; ^{1}H NMR (500 MHz, DMSO-d_6, δ ppm): 6.98 (d, J = 15.7 Hz, 1H), 7.17 (d, J = 7.9 Hz, 1H), 7.41 (t, J = 8.08 Hz, 1H), 7.47 (t, J = 3.65 Hz, 2H), 7.58 (t, J = 4.58 Hz, 1H), 7.82 (t, J = 8.77 Hz, 3H), 7.94 (d, J = 8.85 Hz, 1H), 7.99 (d, J = 15.75 Hz, 1H), 8.07 (s, 1H, NH), 8.6 (s, 1H), 8.89 (s, 1H), 9.95 (s, 1H), 10.65 (s, 1H, NHCO). ESI-MS: 435.1 ($C_{23}H_{16}Cl_2N_4O$, $[M+H]^+$). Anal. Calcd for $C_{23}H_{15}Cl_2N_4O$: C, 63.46; H, 3.70; N, 12.87. Found: C, 63.75; H, 3.45; N, 13.01.

4.4.16. (*E*)-*N*-(4-(3-Chlorophenylamino)quinazolin-6-yl)-3-(4-bromophenyl)acrylamide (35)

Mp 289–291 °C; ^{1}H NMR (500 MHz, DMSO-d_6, δ ppm): 6.95 (d, J = 15.75 Hz, 1H), 7.16 (d, J = 8.1 Hz, 1H), 7.41 (t, J = 8.18 Hz, 1H), 7.62 (d, J = 8.55 Hz, 2H), 7.67 (t, J = 5.65 Hz, 3H), 7.82 (d, J = 8.85 Hz, 2H), 7.96 (dd, J_1 = 9 Hz, J_2 = 9 Hz, 1H), 8.07 (s, 1H, NH), 8.6 (s, 1H), 8.82 (s, 1H), 9.95 (s, 1H), 10.56 (s, 1H, NHCO). ESI-MS: 478.1 ($C_{23}H_{16}BrClN_4O$, $[M+H]^+$). Anal. Calcd for $C_{23}H_{15}BrClN_4O$: C, 57.58; H, 3.36; N, 11.68. Found: C, 57.23; H, 3.36; N, 11.89.

4.4.17. (*E*)-*N*-(4-(3-Chlorophenylamino)quinazolin-6-yl)-3-(2-bromophenyl)acrylamide (36)

Mp 292–293 °C; ^{1}H NMR (500 MHz, DMSO-d_6, δ ppm): 7.38–7.43 (m, 2H), 7.51 (d, J = 7.5 Hz, 1H), 7.75 (d, J = 8.05 Hz, 1H), 7.79–7.84 (m, 3H), 7.94 (t, J = 11.98 Hz, 2H), 8.06 (s, 1H, NH), 8.61 (s, 1H), 8.91 (s, 1H), 9.98 (s, 1H), 10.67 (s, 1H, NHCO). ESI-MS: 479.0 ($C_{23}H_{16}BrClN_4O$, $[M+H]^+$). Anal. Calcd for $C_{23}H_{15}BrClN_4O$: C, 57.58; H, 3.36; N, 11.68. Found: C, 57.83; H, 3.21; N, 11.33.

4.4.18. (*E*)-*N*-(4-(3-Chlorophenylamino)quinazolin-6-yl)-3-(3-methoxyphenyl)acrylamide (37)

Mp 284–285 °C; ^{1}H NMR (500 MHz, DMSO-d_6, δ ppm): 3.82 (s, 3H, OCH_3), 6.93 (d, J = 15.55 Hz, 1H), 7.01 (dd, J_1 = 8.25 Hz, J_2 = 8.25 Hz, 1H), 7.17 (d, J = 7.45 Hz, 1H), 7.64 (d, J = 15.7 Hz, 1H), 7.82 (d, J = 8.85 Hz, 2H), 7.37–7.43 (m, 2H), 7.24 (t, J = 9.3 Hz, 2H), 7.95 (t, J = 5.5 Hz, 1H), 8.06 (s, 1H, NH), 8.6 (s, 1H), 8.85 (s, 1H), 9.97 (s, 1H), 10.54 (s, 1H, NHCO). ESI-MS: 431.1 ($C_{24}H_{19}ClN_4O_2$, $[M+H]^+$). Anal. Calcd for $C_{24}H_{18}ClN_4O_2$: C, 66.90; H, 4.44; N, 13.00. Found: C, 66.84; H, 3.99; N, 13.16.

4.4.19. (*E*)-*N*-(4-(3-Chlorophenylamino)quinazolin-6-yl)-3-(thiophen-2-yl)acrylamide (38)

Mp 241–243 °C; ^{1}H NMR (500 MHz, DMSO-d_6, δ ppm): 6.69 (d, J = 8.5 Hz, 1H), 7.16–7.17 (m, 2H), 7.41 (t, J = 8.1 Hz, 1H), 7.49 (d, J = 3.35 Hz, 1H), 7.69 (d, J = 5 Hz, 1H), 7.82 (d, J = 7.62 Hz, 3H), 7.92 (dd, J_1 = 9 Hz, J_2 = 8.85 Hz, 1H), 8.06 (s, 1H, NH), 8.59 (s, 1H), 8.84 (s, 1H), 9.97 (s, 1H), 10.52 (s, 1H, NHCO). ESI-MS: 451.0 ($C_{21}H_{15}ClN_4OS$, $[M+H]^+$). Anal. Calcd for $C_{21}H_{14}ClN_4OS$: C, 61.99; H, 3.72; N, 13.77. Found: C, 61.83; H, 3.94; N, 13.63.

4.4.20. (*E*)-*N*-(4-(3-Chlorophenylamino)quinazolin-6-yl)-3-p-tolylacrylamide (39)

Mp 277–279 °C; ^{1}H NMR (500 MHz, DMSO-d_6, δ ppm): 2.35 (s, 3H, CH_3), 6.87 (d, J = 15.75 Hz, 1H), 7.16 (d, J = 8.05 Hz, 1H), 7.28 (d, J = 7.9 Hz, 2H), 7.41 (t, J = 8.15 Hz, 1H), 7.55 (d, J = 8.1 Hz, 2H), 7.64 (d, J = 15.7 Hz, 1H), 7.82 (d, J = 8.7 Hz, 2H), 7.95 (dd, J_1 = 9 Hz, J_2 = 8.85 Hz, 1H), 8.06 (s, 1H, NH), 8.6 (s, 1H), 8.83 (s, 1H), 9.95 (s, 1H), 10.5 (s, 1H, NHCO). ESI-MS: 415.1 ($C_{24}H_{19}ClN_4O$, $[M+H]^+$). Anal. Calcd for $C_{24}H_{18}ClN_4O$: C, 69.48; H, 4.62; N, 13.50. Found: C, 69.03; H, 4.57; N, 13.83%

4.4.21. (*E*)-*N*-(4-(3-Chlorophenylamino)quinazolin-6-yl)-3-(naphthalen-4-yl)acrylamide (40)

Mp 293–294 °C; ^{1}H NMR (500 MHz, DMSO-d_6, δ ppm): 7.01 (d, J = 15.4 Hz, 1H), 7.17 (d, J = 9.15 Hz, 1H), 7.42 (t, J = 8.1 Hz, 1H), 7.60–7.69 (m, 3H), 7.85 (d, J = 9 Hz, 2H), 7.9 (d, J = 7.15 Hz, 1H), 7.99–8.05 (m, 3H), 8.26 (d, J = 8.4 Hz, 1H), 8.46 (d, J = 15.55 Hz, 1H), 8.08 (s, 1H, NH), 8.62 (s, 1H), 8.9 (s, 1H), 10 (s, 1H), 10.65 (s, 1H, NHCO). ESI-MS: 495.0 ($C_{27}H_{19}ClN_4O$, $[M+H]^+$). Anal. Calcd for $C_{27}H_{18}ClN_4O$: C, 71.92; H, 4.25; N, 12.43. Found: C, 71.99; H, 4.16; N, 12.51.

4.4.22. (*E*)-*N*-(4-(3-Chlorophenylamino)quinazolin-6-yl)-3-(4-nitrophenyl)acrylamide (41)

Mp 280–282 °C; ^{1}H NMR (300 MHz, DMSO-d_6, δ ppm): 7.42 (t, J = 8.06 Hz, 1H), 7.08–7.18 (m, 2H), 7.75–7.85 (m, 3H), 7.92–8.06 (m, 4H), 8.31 (d, J = 8.4 Hz, 1H), 8.61 (s, 1H), 8.84 (s, 1H), 10 (s, 1H), 10.7 (s, 1H, NHCO). ESI-MS: 446.1 ($C_{23}H_{16}ClN_5O_3$, $[M+H]^+$). Anal. Calcd for $C_{23}H_{15}ClN_5O_3$: C, 61.96; H, 3.62; N, 15.71. Found: C, 61.64; H, 3.38; N, 15.91.

4.4.23. (*E*)-*N*-(4-(3-Chlorophenylamino)quinazolin-6-yl)-3-(2-nitrophenyl)acrylamide (42)

Mp 287–289 °C; ^{1}H NMR (500 MHz, DMSO-d_6, δ ppm): 6.91 (d, J = 15.4 Hz, 1H), 7.17 (d, J = 7.9 Hz, 1H), 7.42 (t, J = 8.07 Hz, 1H), 7.68–7.72 (m, 1H), 7.82–7.88 (m, 4H), 7.93 (d, J = 9 Hz, 1H), 7.97 (d, J = 15.55 Hz, 1H), 8.07 (s, 1H, NH), 8.11 (d, J = 10 Hz, 1H), 8.6 (s, 1H), 8.9 (s, 1H), 9.96 (s, 1H), 10.68 (s, 1H, NHCO). ESI-MS: 446.1 ($C_{23}H_{16}ClN_5O_3$, $[M+H]^+$). Anal. Calcd for $C_{23}H_{15}ClN_5O_3$: C, 61.96; H, 3.62; N, 15.71. Found: C, 61.65; H, 3.38; N, 15.93.

4.4.24. (*E*)-*N*-(4-(3-Bromophenylamino)quinazolin-6-yl)-3-(3-nitrophenyl)acrylamide (43)

Mp 285–286 °C; ^{1}H NMR (300 MHz, DMSO-d_6, δ ppm): 7.12 (d, J = 15.9 Hz, 1H), 7.29–7.42 (m, 2H), 7.74–7.88 (m, 4H), 7.96 (dd, J_1 = 8.97 Hz, J_2 = 8.94 Hz, 1H), 8.12 (d, J = 7.86 Hz, 1H), 8.18 (s, 1H, NH), 8.27 (dd, J_1 = 8.22 Hz, J_2 = 8.25 Hz, 1H), 8.51 (s, 1H), 8.61 (s, 1H), 8.87 (s, 1H), 10.04 (s, 1H), 10.64 (s, 1H, NHCO). ESI-MS: 490.0 ($C_{23}H_{16}BrN_5O_3$, $[M+H]^+$). Anal. Calcd for $C_{23}H_{16}BrN_5O_3$: C, 56.34; H, 3.29; N, 14.28. Found: C, 56.65; H, 3.48; N, 13.91.

4.4.25. (*E*)-*N*-(4-(3-Chlorophenylamino)quinazolin-6-yl)-3-(3-nitrophenyl)acrylamide (44)

Mp 296–298 °C; ^{1}H NMR (300 MHz, DMSO-d_6, δ ppm): 7.08–7.18 (m, 2H), 7.42 (t, J = 8.15 Hz, 1H), 7.66–7.85 (m, 4H), 7.96 (d, J = 8.97 Hz, 1H), 8.07 (s, 1H, NH), 8.13 (d, J = 7.86 Hz, 1H), 8.29 (t, J = 8.13 Hz, 1H), 8.52 (s, 1H), 8.61 (s, 1H), 8.86 (s, 1H), 10.00 (s, 1H), 10.65 (s, 1H, NHCO). ESI-MS: 446.1 ($C_{23}H_{16}ClN_5O_3$, $[M+H]^+$). Anal. Calcd for $C_{23}H_{15}ClN_5O_3$: C, 61.96; H, 3.62; N, 15.71. Found: C, 62.25; H, 3.18; N, 15.69.

4.5. Cell proliferation assay

The antiproliferative activities of cinnamic acid quinazoline amide derivatives were determined using a standard (MTT)-based colorimetric assay (Sigma). Briefly, cell lines were seeded at a density of 7×10^3 cells/well in 96-well microtiter plates (Costar). After 24 h, exponentially growing cells were exposed to the indicated compounds at final concentrations ranging from 0.01 to 100 μg/ml. After 48 h, cell survival was determined by the addition of an MTT solution (20 μL of 5 mg/mL MTT in PBS). After 6 h, 100 mL of 10% SDS in 0.01 N HCl was added, and the plates were incubated at 37 °C for a further 4 h; optical absorbance was measured at 570 nm on an LX300 Epson Diagnostic microplate reader. Survival ratios are expressed in percentages with respect to untreated cells. IC_{50} values were determined from replicates of 6 wells from at least two independent experiments.

4.6. General procedure for preparation, purification of EGFR inhibitory assay

A 1.6 kb cDNA encoded for the EGFR cytoplasmic domain (EGFR-CD, amino acids 645–1186) were cloned into baculoviral expression vectors pBlueBacHis2B and pFASTBacHTc (Huakang Company China), separately. A sequence that encodes $(His)_6$ was located at the 5' upstream to the EGFR sequences. Sf-9 cells were infected for 3 days for protein expression. Sf-9 cell pellets were solubilized at 0 °C in a buffer at pH 7.4 containing 50 mM HEPES,

10 mM NaCl, 1% Triton, 10 μM ammonium molybdate, 100 μM sodium vanadate, 10 μg/mL aprotinin, 10 μg/mL leupeptin, 10 μg/mL pepstatin, and 16 μg/mL benzamidine HCl for 20 min followed by 20 min centrifugation. Crude extract supernatant was passed through an equilibrated Ni-NTA superflow packed column and washed with 10 mM and then 100 mM imidazole to remove non-specifically bound material. Histidine tagged proteins were eluted with 250 and 500 mM imidazole and dialyzed against 50 mM NaCl, 20 mM HEPES, 10% glycerol, and 1 μg/mL each of aprotinin, leupeptin, and pepstatin for 2 h. The entire purification procedure was performed at 4 °C or on ice.[26]

The EGFR kinase assay was set up to assess the level of autophosphorylation based on DELFIA/Time-Resolved Fluorometry. Compounds **20–44** were dissolved in 100% DMSO and diluted to the appropriate concentrations with 25 mM HEPES at pH 7.4. In each well, 10 μL compound was incubated with 10 μL (5 ng for EGFR) recombinant enzyme (1:80 dilution in 100 mM HEPES) for 10 min at room temperature. Then, 10 μL of 5 × buffer (containing 20 mM HEPES, 2 mM $MnCl_2$, 100 μM Na_3VO_4, and 1 mM DTT) and 20 μL of 0.1 mM ATP-50 mM $MgCl_2$ were added for 1 h. Positive and negative controls were included in each plate by incubation of enzyme with or without ATP-$MgCl_2$. At the end of incubation, liquid was aspirated, and plates were washed three times with wash buffer. A 75 μL (400 ng) sample of europiumlabeled anti-phosphotyrosine antibody was added to each well for another 1 h of incubation. After washing, enhancement solution was added and the signal was detected by Victor (Wallac Inc.) with excitation at 340 nm and emission at 615 nm. The percentage of autophosphorylation inhibition by the compounds was calculated using the following equation: 100% − [(negative control)/(positive control − negative control)]. The IC_{50} was obtained from curves of percentage inhibition with eight concentrations of compound. As the contaminants in the enzyme preparation are fairly low, the majority of the signal detected by the anti-phosphotyrosine antibody is from EGFR.

4.7. Molecular docking modeling

Molecular docking of compound **32**, **42**, **43** and Erlotinib into the three-dimensional EGFR complex structure (1M17.pdb, downloaded from the PDB) was carried out using the AutoDock software package (version 4.0) as implemented through the graphical user interface Auto-Dock Tool Kit (ADT 1.4.6).

Acknowledgment

This work was supported by National Basic Research Program of China (2010CB126104), National Natural Science Foundation of China (30901854), and Jiangsu National Science Foundation (BK2009239).

References and notes

1. Modjtahedi, H.; Dean, C. *Int. J. Oncol.* **1994**, *4*, 277.
2. Bridges, A. J. *Curr. Med. Chem.* **1996**, *3*, 167.
3. Fry, D. W. *Annu. Rep. Med. Chem.* **1996**, *31*, 151.
4. (a) Traxler, P. M. *Exp. Opin. Ther. Pat.* **1997**, *7*, 571; (b) *Exp. Opin. Ther. Pat.* **1998**, *8*, 1599.
5. Fry, D. W.; Kraker, A. J.; McMichael, A.; Ambroso, L. A.; Nelson, J. M.; Leopold, W. R.; Connors, R. W.; Bridges, A. J. *Science* **1994**, *265*, 1093.
6. Ward, W. H. J.; Cook, P. N.; Slater, A. M.; Davies, D. H.; Holdgate, G. A.; Green, L. R. *Biochem. Pharmacol.* **1994**, *48*, 659.
7. Bridges, A. J.; Zhou, H.; Cody, D. R.; Rewcastle, G. W.; McMichael, A.; Showalter, H. D. H.; Fry, D. W.; Kraker, A. J.; Denny, W. A. *J. Med. Chem.* **1996**, *39*, 267.
8. Wakeling, A. E.; Barker, A. J.; Davies, D. H.; Brown, D. S.; Green, L. R.; Cartlidge, S. A.; Woodburn, J. R. *Breast Cancer Res. Treat* **1996**, *38*, 67.
9. Fry, D. W.; Nelson, J. M.; Slintak, V.; Keller, P. R.; Rewcastle, G. W.; Denny, W. A.; Zhou, H.; Bridges, A. J. *Biochem. Pharmacol.* **1997**, *54*, 877.
10. Iwata, K.; Miller, P. E.; Barbacci, E. G.; Arnold, L.; Doty, J.; DiOrio, C. I.; Pustilnik, L. R.; Reynolds, M.; Thelemann, A.; Sloan, D.; Moyer, J. D. *Proc. Am. Assoc. Cancer Res.* **1997**, *38*, 633. Abstract 4248.
11. Woodburn, J. R.; Barker, A. J.; Gibson, K. H.; Ashton, S. E.; Wakeling, A. E.; Curry, B. J.; Scarlett, L.; Henthorn, L. R. *Proc. Am. Assoc. Cancer Res.* **1997**, *38*, 633. Abstract 4251.
12. *Company Press Release*, Feb 1, **2010**: GSK's TYKERB receives accelerated approval for first-line combination treatment of hormone receptor positive, HER2+/ErbB2+ metastatic breast cancer.
13. Kavitha, J.; Vanisree, M.; Subbaraju, G. V. *Indian J. Chem.* **2000**, *40*, 522.
14. Chan, R. I.; San, R. H.; Stich, H. F. *Cancer Lett.* **1986**, *31*, 27.
15. Chen, H.; Muramato, K.; Yamauchi, F.; Nokihara, K. *J. Agric. Food Chem.* **1996**, *44*, 2619.
16. Laranjinha, J.; Vierira, O.; Almeida, L.; Madeira, V. *Biochem. Pharmacol.* **1996**, *51*, 395.
17. Mariano, C.; Marder, M.; Blank, V. C.; Roguin, L. P. *Bioorg. Med. Chem.* **2006**, *14*, 2966.
18. Han, C. K.; Ahn, S. K.; Choi, N. S.; Hong, R. K.; Moon, S. K.; Chun, H. S.; Lee, S. J.; Kim, J. W.; Hong, C. I.; Kim, D.; Yoon, J. H.; No, K. T. *Bioorg. Med. Chem. Lett.* **2000**, *10*, 39.
19. Dallavalle, S.; Cincinelli, R.; Nannei, R.; Merlini, L.; Morini, G.; Penco, S.; Pisano, C.; Vesci, L.; Barbarino, M.; Zuco, V.; Cesare, M. D.; Zunino, F. *Eur. J. Med. Chem.* **2009**, *44*, 1900.
20. Qian, Yong; Zhang, Hong-Jia; Zhang, Hao *Bioorg. Med. Chem.* **2010**, *18*, 4991.
21. Thompson, A. M.; Murray, D. K.; Elliott, W. L.; Fry, D. W.; Nelson, J. A.; Showalter, H. D. H.; Roberts, B. J.; Vincent, P. W.; Denny, W. A. *J. Med. Chem.* **1997**, *40*, 3915.
22. Rewcastle, G. W.; Murray, D. K.; Elliott, W. L.; Fry, D. W.; Howard, C. T.; Nelson, J. M.; Roberts, B. J.; Vincent, P. W.; Showalter, H. D. H.; Winters, R. T.; Denny, W. A. *J. Med. Chem.* **1998**, *41*, 742.
23. Rachid, Z.; Brahimi, F.; Katsoulas, A.; Teoh, N.; Jean-Claude, B. J. *J. Med. Chem.* **2003**, *46*, 4313.
24. The Combi-Targeting Concept: Synthesis of Stable Nitrosoureas Designed to Inhibit the Epidermal Growth Factor Receptor (EGFR). *J. Med. Chem.* **2006**, *49*, 3544.
25. Furniss, B. S.; Hannaford, H. J.; Smith, P. W. G.; Tatchell, A. R. *Vogel's Text Book of Practical Organic Chemistry ELBS*, 5th ed.; Bath Press: UK, 1989. p 1040.
26. Tsou, H. R.; Mamuya, N.; Johnson, B. D.; Reich, M. F.; Gruber, B. C.; Ye, F.; Nilakantan, R.; Shen, R.; Discafani, C.; DeBlanc, R.; Davis, R.; Koehn, F. E.; Greenberger, L. M.; Wang, Y. F.; Wissner, A. *J. Med. Chem.* **2001**, *44*, 2719.